2D MODELLING OF SEISMIC WAVE PROPAGATION THROUGH A SOFT SOIL BASIN: KINBURN, CANADA

Stephen Crane
Department of Earth Sciences, Carleton University, Canada
stephen.crane@carleton.ca

Dariush Motazedian
Department of Earth Sciences, Carleton University, Canada
Dariush.Motazedian@carleton.ca

James Hunter
Geological Survey of Canada, Canada
James.Hunter@NRCan-RNCan.gc.ca

ABSTRACT: A tightly spaced array of seismographs has been installed in place to record earthquake ground motions within a soft soil basin near Kinburn, Ontario, Canada. The basin is roughly oval shaped with axes lengths of 7km x 5km and about 140 m in depth at its deepest point. It has been filled with sediments, which have been measured to be very slow, with shear wave velocities between 80 to 200 m/s. The sediments are located above a Precambrian and Paleozoic bedrock, with an average shear wave velocity of roughly 2700 m/s. This high contrast leads to large amplifications in ground motions, however recorded weak motions from the array are much larger than predictions using one dimensional soil profiles. This study implements two dimensional cross sections of the basin along it's long and short axes, into the spectral element method software, SPECFEM2D. This is used to numerically simulate seismic wave propagation from the seismic source through the basin. An array of receivers, both on the surface, and throughout the basin, are used to determine the transfer of waves into the soft soil basin. Using the receivers from the simulations, along with early recordings from the seismic array, we are able to compare the amplification of weak ground motions from the bedrock to the soil. Investigating particle motions and relative amplifications from horizontal and vertical movements in both the bedrock and soil, we have determined the transfer function between the two.

1. Introduction

The strength and amplitude of seismic waves can vary rapidly over a small distance with a strong dependence on the depth of overlying soil through which they are travelling. Predicting levels of shaking is critical for the design and building of infrastructure in both highly populated and sparsely populated regions. The high variation of seismic wave strength creates a difficult challenge for seismologists to predict levels of ground shaking even over a small region, for the purpose of estimating the seismic hazard in an area. Furthermore, there are certain areas which knowing the soil depth and its properties may not be enough for an accurate prediction of seismic amplitudes and durations.

The city of Ottawa, Canada and the surrounding region is one of the areas where there is a drastic change in seismic wave amplitudes from one location to another. There have been recorded instances of weak ground motion being amplified in soil up to 40 times stronger than a recording in bedrock less than two kilometres away (Hunter *et al.* 2010, Motazedian *et al.*, 2011). It is important to be able to distinguish between these two areas, since a structure which is resistant to a certain level of seismic shaking may not be suitable a short distance away. There has been a large effort to classify the

areas which are at higher risk in the Ottawa region (Hunter *et al.* 2010; Motazedian *et al.,* 2011), which is based on the National Building Code of Canada (NBCC) seismic class list. Certain areas which have a high risk associated with them are due to underlying valley or basin structures in the bedrock, which have been filled with soft sediments. Several of these, which were identified during the seismic microzonation mapping project (Hunter *et al.* 2010, Motazedian *et al.*, 2011), were mapped further using several different methods to get a better constraint on the shape of the underlying bedrock.

The spectral element method is a common tool for solving elastic wave propagation through the Earth on both a regional and global scale (Komatitsch et al., 1999; Krishnan *et al.*, 2012; Monteiller *et al.,* 2013; Magoni *et al.,* 2014, for example). This method, described in detail by Komatitsch and Tromp (1999) for three-dimensional seismic wave propagation, uses a spectral solution for solving the equations of motion over a volume which is subdivided into a number of elements. This method is solved in two dimensions by using as surface elements as the volume and edges as boundary elements (Komatitsch *et al.* 1999; Komatitsch et al. 2001). Applying the spectral element technique to the basin in Ottawa is a unique challenge because of a large contrast between the bedrock and soil.

For this article, a 2-D version of this method was applied to the Kinburn basin in two different profiles, along both of the axes of the basin. Both profiles had several stations of the Kinburn Seismic array within their boundaries, which created simulated recordings at those locations. Using these recordings different wave types were identified through particle motion plots, and theoretical transfer functions were produced for different soil depths and different locations in the basin. This provides a platform for assessing the seismic hazard throughout the basin.

2. Kinburn Basin

2.1. Kinburn Basin Model

East of Kinburn, a part of western Ottawa, there is a roughly oval shaped basin filled with Holocene aged soft sediments, and areas of thin Pleistocene aged glacial deposits. The Pleistocene glacial sediments vary in thickness, but are usually limited to less than 5 metres thick, with certain narrow buried valleys which could have a possible thick layer of about 30-35 metres. The Holocene sediments are soft sediments deposited from the Champlain Sea circa. 15,000-11,000 years ago (Medioli *et al.* 2012). These sediments are up to 120 metres thick in the deepest parts of the basin. The total thickness of Pleistocene plus Holocene sediments in the deepest part of basin is 140m.

Several types of data were collected to constrain the soil depths in the Kinburn basin, shown as contour lines in Figure 1. This data includes: about 320 Horizontal to Vertical Spectral Ratios (HVSR) determined from passive measurements on portable Tromino devices (triangles); a borehole from the Geological Survey of Canada (GSC BH); landstreamer seismic lines (Pugin *et al.*, 2007) along John Shaw rd. and Grants Side rd. (crosses); and roughly 900 city of Ottawa waterwell logs (circles). The soil depth increases rapidly near the centre of the basin and along the Northern and Western edges, with a more gradual slope to the South and East of the basin. Outcrops to the North and Northwest indicate Precambrian bedrock for the Northwest portion of the basin, which is indicated by the steep slopes and sharp changes in soil depth. Further, South there are Paleozoic outcrops, which infer a Paleozoic bedrock in the Southeastern portion of the basin. The slight increase of soil depth South and Eastward have a similar behaviour of the Paleozoic basement rock in the area.

The general basin structure of interest spans roughly 7 km in the Northwest to Southeast direction, starting just South of Kinburn Side Rd. and traversing across John Shaw Rd., almost reaching Thomas A. Dolan Pkwy. The Southwest to Northeast axis is roughly 5 km from Donald B. Munro Dr. to Diamondview Rd. slightly Northwest of Grants Side Rd. Although the soil depth decreases gently in the Southeast and Southwest directions, the main area of focus does not extend as far, since the seismic site class changes to D at a soil depth of about 20 metres and to C at about 10 metres. Calculations of V_{s30} for these and the seismic site classifications are from Benjumea *et al.* (2008). These two axes, the Northwest to Southeast (NW-SE) and Southwest to Northeast (SW-NE) directions, were chosen as the profiles for the 2 dimensional numerical simulations. For these simulations the materials were simplified to bedrock and soil. These materials were described by their average P-wave velocity, average shear wave velocity, average density, and an estimated Q value from previous studies (Hunter et al. 2010, Motazedian et al.,

2011). This simplification of parameters reduces the computing time and memory required for these simulations.
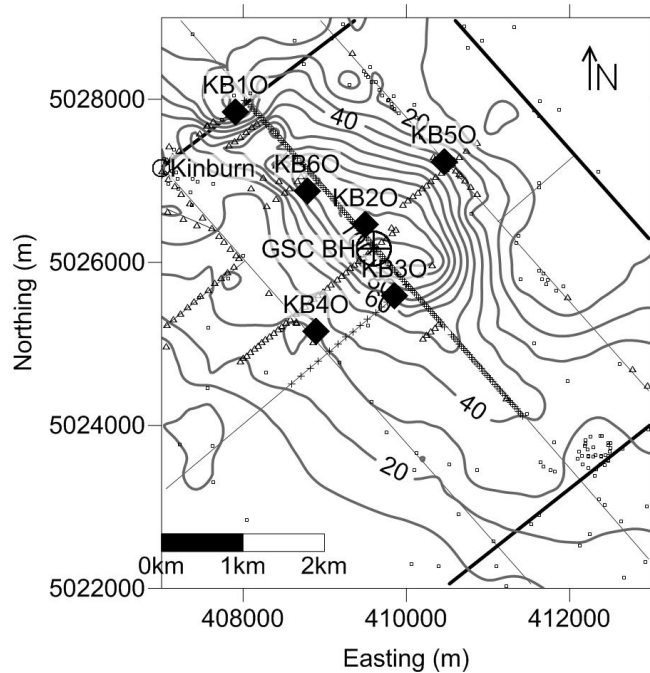
Figure 1 – Contoured soil depth of the Kinburn Basin, the location of the Kinburn Seismic Array, and the GSC borehole. Triangles are HVSR data points, crosses are landstreamer data locations, and open circles are city of Ottawa waterwell locations.

2.2. Kinburn Seismic Array

The Kinburn Seismic Array is a tightly spaced array of broadband seismometers installed at several key locations within the Kinburn basin. These stations are shown in Figure 1 as diamonds and labelled KB1O to KB6O. The station layout and locations were chosen based on locations available and the best possible configuration to capture possible 3 dimensional basin effects, as well as different 1 dimensional soil amplification effects throughout the basin. The soil depths, and the maximum horizontal to vertical spectral ratio, shown in Table 1, were determined from HVSR measurements at the station site before installation. To date the array has recorded several teleseismic events and a few weak motion events.

Table 1 – Kinburn Seismic Array parameters

Station Name	Location in UTM coordinates (Zone 18)		Maximum H/V Frequency (Hz)	Depth to Bedrock (m)
	Northing (m)	Easting (m)		
KB1O	5027845	407908	-	0 (outcrop)
KB2O	5026463	409499	0.72 ± 0.01	101.2 ± 0.9
KB3O	5025592	409855	0.84 ± 0.01	82.0 ± 1.2
KB4O	5025153	408894	1.63 ± 0.01	32.4 ± 0.3
KB5O	5027234	410461	1.31 ± 0.01	54.7 ± 0.7
KB6O	5026876	408786	0.75 ± 0.01	96.0 ± 1.1

2.3. Kinburn basin: NW-SE profile

The NW-SE profile of the Kinburn basin was modeled with the data taken along John Shaw Rd, partially shown in Figure 2a. This includes several HVSR measurements, along with a high-resolution

landstreamer seismic line. The soil depth is well constrained along this direction, and the basin has four stations roughly in line from the Kinburn seismic array.
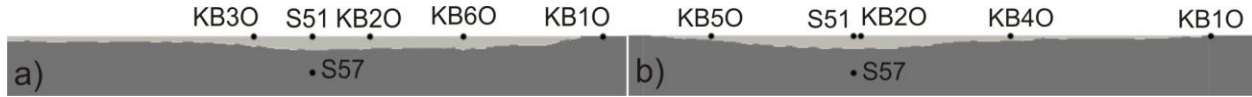
Figure 2 – A close up outlining the Kinburn seismic array stations and soil depth of the basin surrounding those stations for a) the NW-SE profile model used for the numerical simulations; and b) the SW-NE profile model used for the numerical simulations. Each profile shown is 5km across.

There are three simulations which were done with this profile: an incoming plane P-wave travelling upwards; an incoming plane S-wave travelling upwards; and the moment tensor solution corresponding to the Ladysmith M4.6 earthquake of April 17, 2013 (Bent *et al.*, 2015). The model was extended to 20 km depth and 50 km in width to accommodate the distance and depth of the source for the Ladysmith earthquake. The simulations include receivers that are not shown in Figure 2. There were 50 equally spaced between 0 and 10km along the surface of the entire model, along with six receivers between S51, at the surface of the basin at the location of the largest amount of sediments, and S57, about 150 metres below the boundary between sediments and bedrock which is roughly the same distance between the surface and sediment bedrock interface at this location.

2.4. Kinburn basin: SW-NE profile

The SW-NE model of the Kinburn basin, partially shown in Figure 2b, was determined primarily from HVSR measurements taken along that axis of the basin. The soil depth is not constrained as well as the NW-SE profile, since there was little access for high resolution imaging. The HVSR measurements which were taken agree well with the basin structure inferred from other methods. Two simulations were conducted for this model: an incoming plane P-wave travelling upwards; and an incoming S-wave travelling upwards. The simulations also had 50 equally spaced receivers along the surface from 0 to 10km, and 6 equally spaced between S51 and S57.

3. Numerical Simulations

3.1. Plane waves

An incoming plane P-wave and an incoming S-wave propagating upwards were simulated throughout the entire width of the models. The initial P-wave is shown by the arrival of a strong initial vertical component arriving simultaneously at the surface, with a slight delay within the boundaries of the soft soil basin shown in Figure 3. The time delay and amplified initial vertical motion of each receiver corresponds with the soil depth at each location. A snap shot of the incident plane P-wave with vertical propagation, and strong initial reflections can be seen in Figure 4a, displaying the SW-NE profile. Figure 4b shows several snapshots of a vertically propagating S-wave in the NW-SE profile, along with some model edge effects resulting from the boundaries of the model. These are seen as strong wavefronts on the edges outside the basin, but are later arriving than the initial wavefront within the basin.
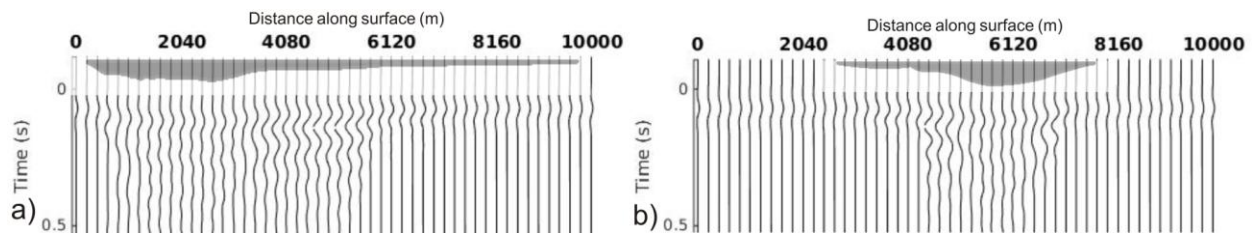
Figure 3 - The vertical component of the acceleration time series for the P-wave source with the soil depth overlay: a) is the NW-SE profile and b) is the SW-NE profile. A band-pass filter was applied with corner frequencies of 0.1 to 5 Hz.
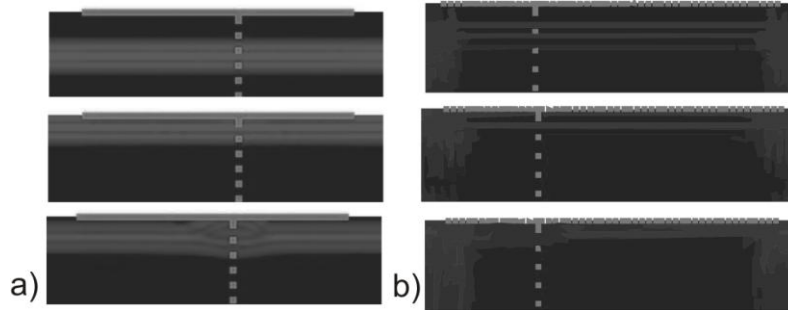
Figure 4 - Snapshots of the normal acceleration in the model. a) SW-NE profile P-wave at -0.2s (top), 0.0s (middle), 0.2s (bottom). b) NW-SE profile S-wave at 1.0s (top), 1.2s (middle), 1.4s (bottom).

There is a strong amplification of the initial wave front through the vertical profile from stations below the soil-rock interface roughly 150m in depth at the borehole receiver line, to the surface within the basin. Both the NW-SE, shown in Figure 5a and Figure 6a, and SW-NE profile, shown in Figure 5b and Figure 6b show this initial amplification. These figures are the recordings from simulations at different depths through a vertical line at the maximum depth of the basin in their respective the profiles. Both of these locations roughly correspond to the position of the station KB2O, the soil station near the centre of the basin, however the position of these borehole receivers were chosen at the location in the model which had the largest sediment depth. The P-wave source displays a strong initial vertical wave front, which then increases through the soil-rock interface. A small amplitude reflection can be seen propagating downwards after the wavefront reaches this boundary. This is seen as a second wavefront which is later arriving in the deeper receivers in both Figure 5 and Figure 6. In the later times of the simulation there is a strong resonating effect in the soil, predominately in seen in depths of 100m or less. Most of these can be attributed to the wave being trapped in the soil basin, however later strong arrivals are seen as reflections from the model boundaries from inefficient boundary conditions.
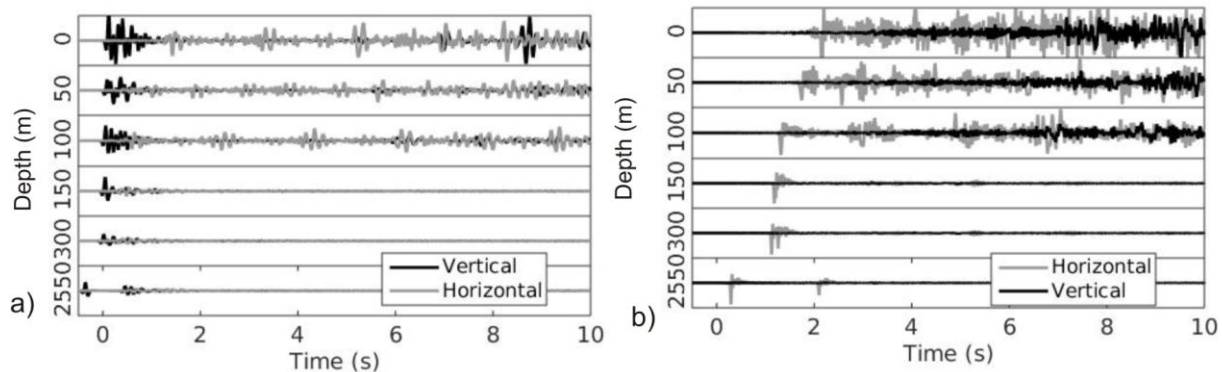
Figure 5 - The time series of the NW-SE profile: a) the P-wave source and b) the S-wave source. A band-pass filter was applied with corner frequencies of 0.1 to 5 Hz.

The particle motion, Figure 7, is plotted for KB2O to try and identify wave types in the basin. The time is limited to 5 seconds to avoid any of the undesired reflections being plotted. Each image is grey scaled to try and show the particle motion from the start to end of each plot. Figure 7a and 7b are the particle motion for the NW-SE profile with initial P-wave and S-wave respectively. Figure 7a shows a predominantly initial vertical component associated with an initial P-wave for both stations and the source. After the initial vertical movement, the vertical and horizontal movement is equal, changing to a dominate horizontal motion after roughly 1.5 seconds. The S-wave source for the NW-SE profile, shown in Figure 7b, displays initial and lasting horizontal movement. This motion has a delayed start, and the only change with time is the strength of the horizontal movement. The SW-NE profiles, displayed in Figure 7c for the P-wave source and Figure 7d for the S-wave source, displays some similar particle motions at each location. The initial P-wave can be seen as a strong vertical movement, which quickly disappears then a lasting horizontal motion in the basin. The S-wave source has an initial vertical motion arriving much

sooner than the anticipated S-wave front. This can be seen in the wavefield snapshots and are likely reflections from the bottom edge of the model. It is difficult to pick out any late arriving wave types from these particle motions, as the dominating later movements are lateral.
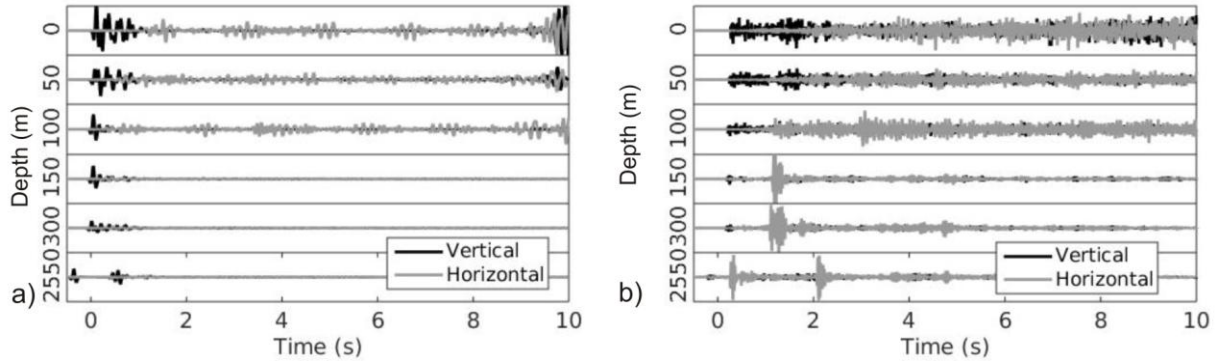
Figure 6 - The time series of the SW-NE profile: a) the P-wave source, and b) the S-wave source. A band-pass filter was applied with corner frequencies of 0.1 to 5 Hz.
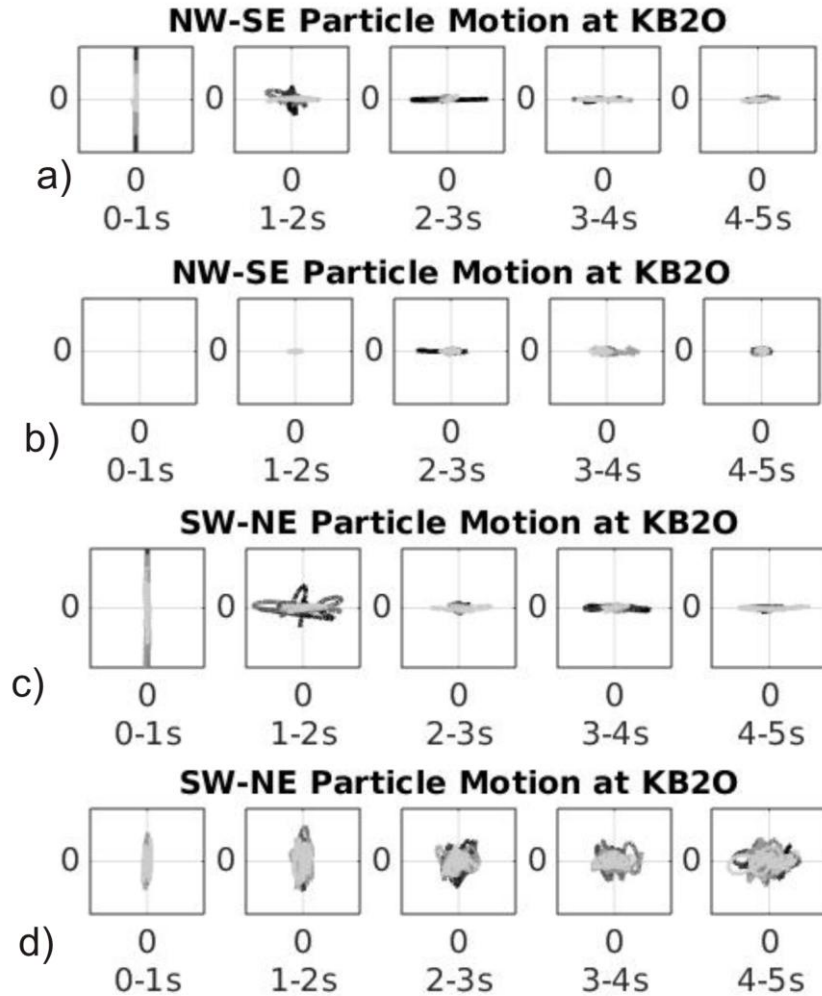
Figure 7 - Particle motion plots for the simulations at KB2O: a) the NW-SE profile plane P-wave; b) the NW-SE profile plane S-wave; c) the SW-NE profile pane P-wave; and d) the SW-NE profile plane S-wave. Each time slice is grey scaled starting with darker colours.

The theoretical transfer functions from the plane wave simulations are shown in Figure 8 and 9 for both the P-wave and S-wave sources. The transfer functions are shown in comparison to the rock station for the Kinburn array, station KB1O. The transfer function between stations S58, 300m below the surface, and S51, at the surface directly above S58 is also shown. The transfer functions show different amplifications at each station depending on the nature of the initial wave and type of motion. There are several peaks which correlate to dominate frequencies within the basin at each station. The soil stations show predominately that the motions are amplified over a wide range of frequencies, occasionally reaching levels of 100 times for peak amplification frequencies. Several of the peaks in the transfer functions correspond well to the measured fundamental frequency by the HVSR method. The fundamental site frequency is strongly dependent on sediment depth and is the frequency at which the strongest resonance amplification is present. In this area, the common site frequencies are less than 1.5Hz which can have a devastating effect on structures with similar natural frequencies. The presence of these fundamental frequencies in the models is an indication that some of the important factors for seismic hazard assessment are being met from this modelling. Knowing the site periods at the location of the stations gives a good measuring tool to determine the accuracy of the models for determining the site periods in the basin.
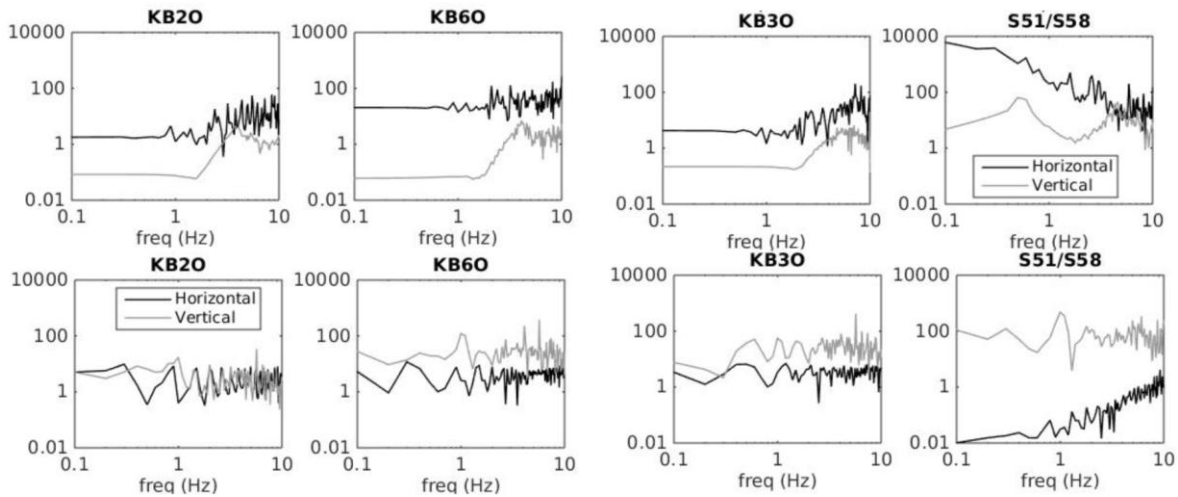
Figure 8 - Theoretical transfer functions for different sites in the NW-SE profile for the horizontal and vertical components. Top is the incident P-wave source, bottom is the incident S-wave source.
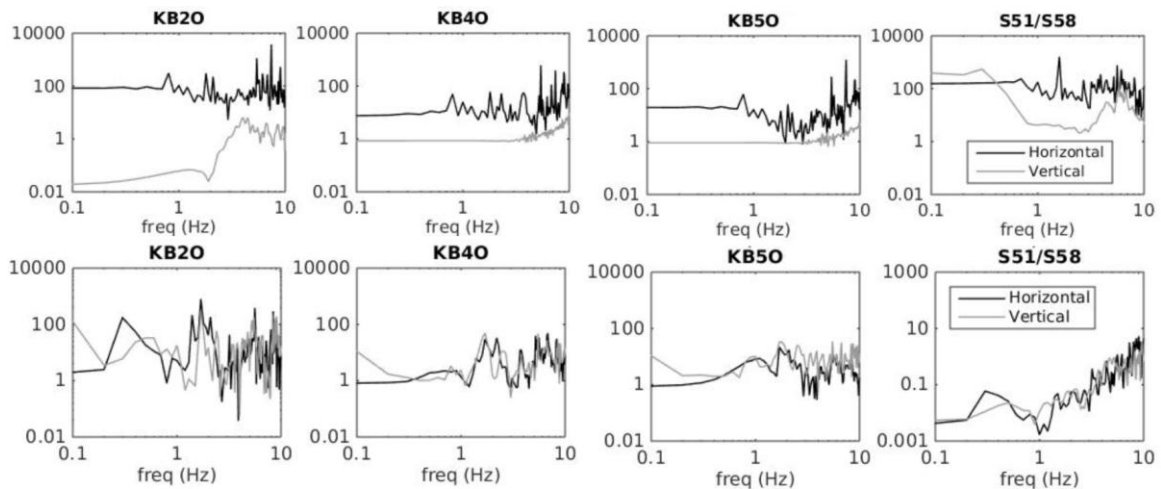
Figure 9 - Theoretical transfer functions for different sites in the SW-NE profile for the horizontal and vertical components. Top is the incident P-wave source, bottom is the incident S-wave source.

3.2. Ladysmith Earthquake

The Ladysmith earthquake occurred on April 17th, 2013 about 18 kilometres Northeast of Shawville Quebec, had a measured moment magnitude of 4.6 and a depth of roughly 14 km (Bent *et al.*, 2015). At the time of the earthquake there were two stations recording in the Kinburn basin. Station 1 was JSBS, now KB1O, recorded the motion on a bedrock outcrop, while the other station, JSSS, now KB2O, recorded the motions on a soil site near the centre of the basin. Figure 10 shows the recorded acceleration time series for the horizontal North-South and vertical motions for both stations. As can be seen, the amplitude of the accelerations recorded at the soil station is much greater than the ones recorded at the rock station. The moment tensor solution corresponding to the Ladysmith earthquake source (Bent *et al.*, 2015) was used as the input for the model, and the simulated acceleration time series at both the soil and rock stations were obtained, as shown in Figure 11. The shapes of the simulated acceleration time series in the time domain do not strictly follow the shape of recorded acceleration time series for the stations. There are several reasons for this, the main one being the input for the model is overly simplified for the region. Most of the path effects are not present as the model is homogeneous from the source to the basin and receivers. The basin itself has been shown to have a strong influence on the motions due to the soil profile (Hayak et al. 2015). The amplification from the rock to soil station is seen to be much similar in the simulations, however the strong motion durations are much longer in the simulations. This is a significant concern for using these simulations, and more research will be completed in order to constrain and justify the parameters used. Although the amplitudes are not matched from simulation to recording in spectral domain shown in Figure 12, the spectral shape seems to be somewhat preserved in the simulations. Figure 12 shows the spectral content of both the recordings and simulations at the bedrock and soil for the horizontal and vertical directions when comparing the NW-SE profile to the recorded data. The transfer function between KB2O and KB1O is shown in Figure 13 for the recorded and simulated motions for the NW-SE profile, which match very closely for frequencies above 0.3Hz. This is an indication that the model of the soil basin is producing some of the desired effects which occur within this basin.
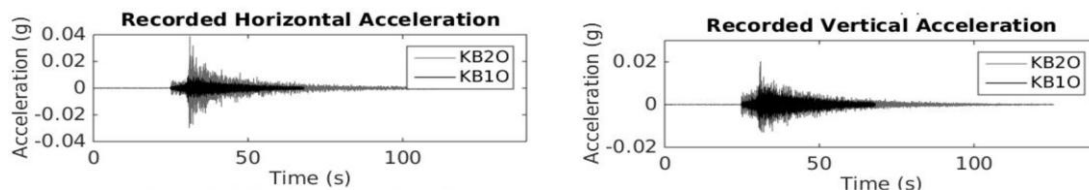
Figure 10 - Recorded horizontal and vertical acceleration time series for the Ladysmith earthquake.
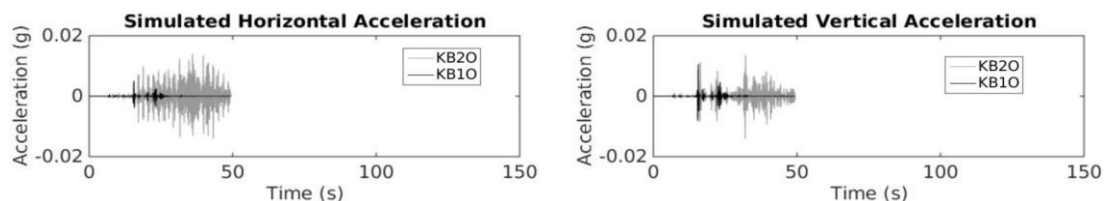
Figure 11 - Simulated horizontal and vertical acceleration time series for the Ladysmith earthquake.

4. Discussion

The spectral element method provided a useful tool for simulating wave propagation through the soft soil filled Kinburn basin. Although the 2-D simulation using this method captured the recorded amplification levels in time domain, the levels of the spectral content of the propagating waves did not match up. The theoretical transfer functions provide a useful guideline for amplification within the basin. The particle motion plots from the simulated recordings show that there are different types of waves being generated as the wavefronts reach the sediment-bedrock boundary throughout the basin, however it is hard to distinguish the types of waves being generated. These generated waves could account for levels of amplification seen within the basin that are not accounted for using one dimensional soil profile methods. These generated waves also appear to affect the areas surrounding the basin as well.
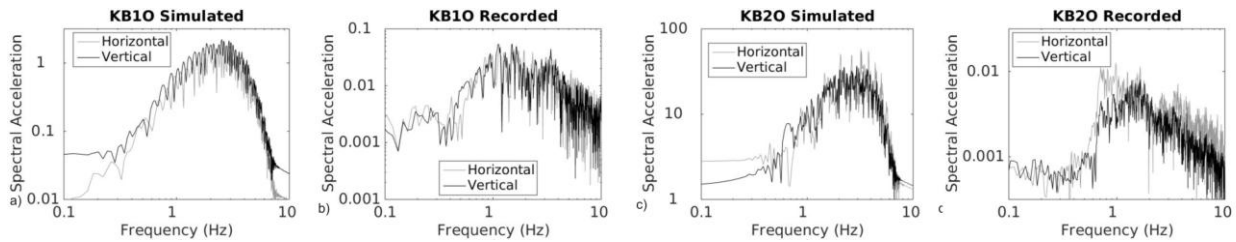
Figure 12 - Spectral accelerations for NW-SE profile for the Ladysmith earthquake, for both the simulated and recorded data.

Although there are limited recordings of earthquakes from the Kinburn Seismic array to date, we were able to use past recordings of a soil and rock station pair in the area to compare them with the simulations. This comparison was mainly useful in the frequency domain, when comparing the transfer functions between rock and soil stations. Future recordings from the array and 3-D simulations will allow us a better comparison throughout the entire basin, not just the edge and centre. Although this area is not affected by local earthquakes often, the array does record unique signature from teleseismic events. Mostly resonance effects are seen from these, but the resonance is unique at each location and matches the resonance peaks recorded by the HVSR method to a good degree.
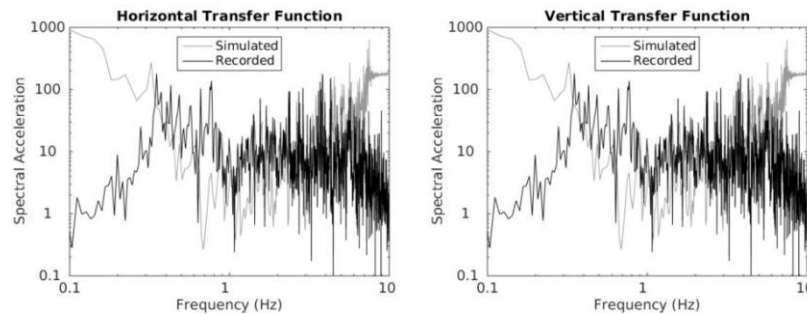
Figure 13 - Transfer functions for the horizontal (left) and vertical (right) components between KB2O and KB1O for the NW-SE profile for both the simulated and recorded Ladysmith earthquake.

The two dimensional numerical simulations in this basin provided the framework for assessing seismic hazard throughout the basin. One dimensional methods were able to capture strong amplifications in the basin, however they failed to produce the same amount of amplification seen in the recordings. Combining both methods will help to get simulated amplitudes closer to expected values within the basin from local earthquakes which are possible in the area. Using this method in other similar basins will help with a more accurate classification of seismic hazard in these basin structures. Determining the fundamental frequencies throughout the basin, at different soil depths and subsurface structures, will help with the mitigation efforts for damage as a result from local earthquakes. Even though the 2-D models preformed well matching the spectral content of the propagating waves, the models still lacked significant 3-D effects seen in the recordings. 3-D modelling of this basin is ongoing using the 3-D version of the spectral element method.

5. Acknowledgements

6. References

Benjumea, Beatriz, Hunter, James A., Pullan, Susan E., Brooks, Gregory R., Pyne, Matt and Aylsworth, Janice M. " Vs30 and Fundamental Site Period Estimates in Soft Sediments of the Ottawa Valley from Near-Surface Geophysical Measurements" *JEEG*, December 2008, **13**, Issue 4, pp. 313–323.

Bent, A. L., M Lamontagne, V. Peci, S. Halchuk, G. R. Brooks, D. Motazedian, J. A. Hunter, J. Adams, C. Woodgold, J. Drysdale, S. Hayek and W. N. Edwards. "The 17 May 2013 M 4.6 Ladysmith, Quebec, Earthquake", *Seismological Research Letters*, **86**, no. 2, March/April 2015, 460-476.

Hunter, J.A., Crow, H.L., Brooks, G.R., Pyne, M., Motazedian, D., Lamontagne, M., Pugin, A. J.-M., Pullan, S.E., Cartwright,T., Douma, M., Burns, R.A., Good, R.L., Kaheshi-Banab, K., Caron, R., Kolaj, M., Folahan, I., Dixon, L., Dion, K., Duxbury, A ., Landriault, A., Ter-Emmanuil, V., Jones, A., Plastow, G., Muir, D., "Seismic Site Classification and Site Period Mapping in the Ottawa Area Using Geophysical Methods", Geological Survey of Canada, *Open File 6273*, 2010, 1 DVD.

Hayak, S., Hunter, J., Motazedian, D., Audet, P. and Crane, S. "Studies of weak ground motion recordings over soft sediment filled basins in Ottawa, Ontario. *Submitted to 11th Canadian Conference on Earthquake Engineering.*

Komatitsch, Dimitri, Liu, Qinya, Tromp, Jeroen, Süss, Peter, Stidham, Christiane, Shaw, John H., "Simulations of Ground Motion in the Los Angeles Basin Based upon the Spectral-Element Method", *Bull. Seism. Soc. Am.*, **94**, February 2004, 187-206.

Komatitsch, Dimitri and Tromp, Jereon, "Introduction to the spectral element method for three-dimensional seismic wave propagation", *Geophys. J. Int.,* **139**, 1999, 806-822.
Komatitsch, Dimitri and Vilotte, Jean-Pierre and Vai, Rossana and Castillo-Covarrubias, José M. and Sánchez-Sesma, Francisco J. "The spectral element method for elastic wave equations—application to 2-D and 3-D seismic problems", *Int. J. Numer. Meth. Engng.* **45**, 1999, 1139-1164.

Komatitsch, Dimitri and Martin, Roland and Tromp, Jereon and Taylor, Mark A. and Wingate, Beth A. "Wave propagation in 2-D elastic media using a spectral element method with triangles and quadrangles", *Journal Of Computational Acoustics,* **09**, June 2001, 703-718.

Konno, Katsuaki and Ohmachi, Tatsuo. "Ground-motion characteristics estimated from spectral ratio between horizontal and vertical components of microtremor. *Bull. Seism. Soc. Am.*, **88**, February 1998, 228-241.

Krishnan, S. and Casarotti, E. and Goltz, J. and Ji, C. and Komatitsch, D. and Mourhatch, R. and Muto, M. and Shaw, J. H. and Tape, C. and Tromp, J. "Rapid Estimation of Damage to Tall Buildings Using Near Real-Time Earthquake and Archived Structural Simulations", *Bull. Seism. Soc. Am.,,* **102**, December 2012, 2646-2666

Magnoni, F. and Casarotti, E. and Michelini, A. and Piersanti, A. and Komatitsch, D. and Peter, D. and Tromp, J. (2014) "Spectral-Element Simulations of Seismic Waves Generated by the 2009 L'Aquila Earthquake", *Bull. Seism. Soc. Am.,* **104,** February 2014, 73-94.

Medoili, B.E., Aplay, S., Crow, H.L., Cummings, D.I., Hinton, M.J., Knight, R.D., Logan, C., Pugin, A.J.-M., Russell, H.A.J., and Sharpe, D.R., "Integrated data sets from a buried valley borehole, Champlain Sea basin, Kinburn, Ontario", Geological Survey of Canada, *Current Research*, 2012, 16p.

Monteiller, V. and Chevrot, S. and Komatitsch, D. and Fuji, N. "A hybrid method to compute short-period synthetic seismograms of teleseismic body waves in a 3-D regional model", *Geophysical Journal International,* **192**, January 2013, 230-247.

Motazedian D., Hunter, J.A., Pugin, A., Khaheshi Banab, K., and Crow, H.L. "Development of a Vs30 (NEHRP) Map for the City of Ottawa, Ontario, Canada", *Canadian Geotechnical Engineering Journal*, **48**, March 2011, 458-472 doi:10.1139/T10-081.

Pugin, A., Hunter, J.A., Motazedian, D., and Khaheshi Banab, K. "An application of shear wave reflection landstreamer technology to soil response evaluation of earthquake shaking in an urban area, Ottawa, Ontario." SAGEEP Conference Bulletin. Environmental and Engineering Geophysical Society (EEGS), 2007, Denver, Colo.